The theory of fluctuations and texture embryos in structural phase transitions mediated by strain



1994 J. Phys.: Condens. Matter 6 3679

(http://iopscience.iop.org/0953-8984/6/20/008)

J. Phys.: Condens. Matter 6 (1994) 3679–3696. Printed in the UK

# The theory of fluctuations and texture embryos in structural phase transitions mediated by strain

A M Bratkovsky†¶, S C Marais‡, Volker Heine‡ and E K H Salje†§

† Interdisciplinary Research Centre in Superconductivity, Madingley Road, Cambridge CB3 0HE, UK

‡ TCM, Cavendish Laboratory, Madingley Road, Cambridge CB2 0HE, UK

§ Department of Earth Sciences, Downing Street, Cambridge CB2 3EQ, UK

Received 14 January 1994

**Abstract.** Structural phase transitions are considered in which the effective ordering interaction $J(R_{ij})$ arises from local stresses induced by the ordering in cell $i$ and propagated elastically to a distant cell $j$. The generalized Landau free energy functional is set up and four applications made. Firstly the origin of metastable tweed microstructures is shown to lie in the dense medium of strong embryonic tweed-like microdomains existing as fluctuations at temperatures as high as $2T_c$ and above. Secondly the tweed-like pattern originates from the very anisotropic interaction associated with domain walls, and four cases are distinguished. Thirdly it is shown that the Landau–Ginzburg theory of the width and shape of a domain wall can be carried over in some cases but not others. Fourthly the magnitude of critical fluctuations is considered together with corresponding corrections to the Landau theory of the phase transition in the four cases.

## 1. Introduction

The purpose of this paper is to discuss various thermodynamic effects and their implications in systems where the cooperative ordering behaviour is mediated by coupling strain, as in ferroelastic and co-elastic crystals.

Many materials of interest, including perovskites and silicate minerals, show typical structural instabilities generated by strain. The origin of such strain is not always the traditional softening of an acoustic branch, but may be related to some intracell ordering as in many oxide ceramics, high-$T_c$ superconductors, relaxors, etc. The metastable textures often formed in these materials during (dis)ordering have characteristic length scales much larger than a lattice spacing, clearly showing an involvement of long-range elastic forces.

In discussing the origin of the local ordering processes, we have in mind, for example, materials containing rather rigid units such as $BX_4^{2-}$, $NO_2^-$, or $CO_3^{2-}$ ions or a $C_6H_5$ phenyl group, or in other cases the linking of $SiO_4$ tetrahedra (also rather rigid) in framework silicate structures or octahedra in perovskites. This packing and linking of such rigid units results in an ordering interaction $J(R_j)$ in the material [1–4]. When atomic ordering takes place in one cell of the lattice or when one unit rotates at position $R_i$, it inevitably pulls or pushes neighbouring atoms or/and units, i.e. it creates a local displacement field. This field then displaces atoms beyond it and hence it propagates elastically to distant parts $R_j$ of the crystal via a knock-on effect. That distant displacement pattern will act as an effective force field tending to order the crystal around $R_j$. We therefore have an ordering interaction $J(R_{ij})$

¶ Present address: Department of Materials Science, Parks Road, Oxford OX1 3PH, UK.

0953-8984/94/203679+18$19.50  

mediated by strain. For example in figure 1 we show very schematically an ordering of two large and two small atoms on four sites in one unit cell at $\boldsymbol{R}_i$ which will tend to produce a rhombohedral distortion of the cell. When propagated elastically to the cell at $\boldsymbol{R}_i$, that change in cell shape will induce a corresponding ordering of atoms on the four sites there, thus giving the interaction $J(\boldsymbol{R}_{ij})$. We shall call this a strain-mediated interaction. The situation is closely analogous to the Coulomb interaction, with the elastic strain fields here replacing the electrostatic fields, except that our local originating displacement pattern arises from a multipole of vector forces, which is usually more complicated than the multipoles of scalar charges in the electrostatic case. Further we shall confine ourselves to systems where the ferroelastic behaviour is negligible in comparison with the elastic effect, i.e. the dipole–dipole interaction is unimportant.

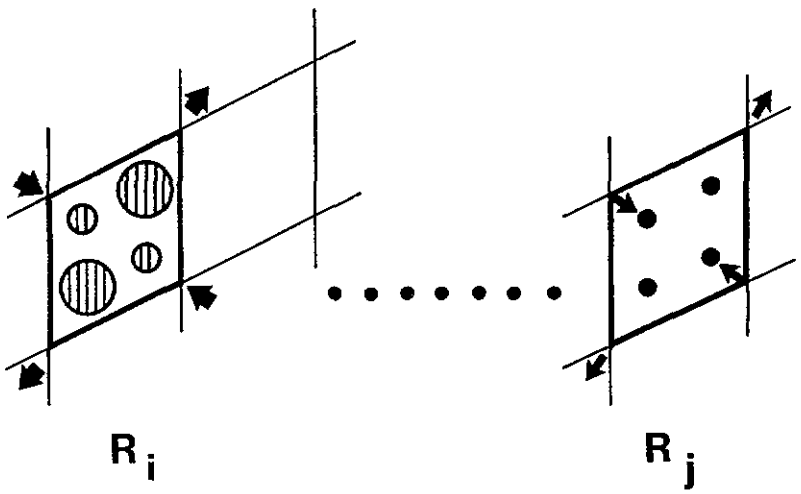


**Figure 1.** An ordering process in cell $i$ on the left (pictured here as the ordering of large and small atoms on four sites) tends to distort the unit cell and to create a local stress field, denoted by four arrows acting on the surroundings. The stress is propagated to distant cells $j$ on the right where a distortion of the cell acts as a force field, tending to order the atoms there.

In a previous paper [1] we have developed the theory of strain-mediated interactions in order to understand various phenomena mentioned briefly below. The crux of the matter lies in the relatively long range of elastic forces and their strong anisotropy. We obtain, broadly speaking:

(i) in the ferroelastic (F) case

$$J(\boldsymbol{R}) \sim \left[A_2 Y_{2m}(\theta,\varphi) + A_4 Y_{4m}(\theta,\varphi)\right]/R^3 + J_Z \qquad (1.1)$$
$$J_Z = Z/N$$

(ii) in the antiferroelastic (AF) case

$$J(\boldsymbol{R}) \sim \left[A_2 Y_{2m}(\theta,\varphi) + A_4 Y_{4m}(\theta,\varphi) + A_6 Y_{6m}(\theta,\varphi)\right]/R^5. \qquad (1.2)$$

Here $Y_{lm}$ represents some appropriate spherical harmonic of order $l$ and the angular term in (1.1) is the strongest one, but of course averages to zero over any shell of radius $R$.

The most anomalous part of (1.1) is the term $-(Z/N)$, which is constant, i.e. has infinite range. It is of order $1/N$ as would be suggested by normalization, where $N$ is the number of crystal cells in the specimen. It is a Zener–Eshelby type of force [5, 6] and is related to the macroscopic change of shape of a domain on undergoing the phase transition. Although the Zener–Eshelby term is of order $1/N$, it gives a finite contribution to $T_c$ and to the enthalpy per mole of the phase transition, when summed over all cells. It is also responsible for some of the phenomena to be mentioned below. We shall hereafter refer to it as the Zener or 'volume' term or interaction, to denote that it extends with infinite range throughout the volume of the material. In fact it depends on $\boldsymbol{R}_i$, $\boldsymbol{R}_j$ and the shape of the boundary and is sometimes called an image force by analogy to electrostatics, but it has a unique non-zero average value denoted by $-Z/N$, which our theory derived [1]. There is also a second interesting feature of our results. In the ferroelastic case the interaction in Fourier transform $J_k$ has a singularity at $\boldsymbol{k} = \boldsymbol{0}$ in that the limit of $J_k \to 0$ depends on the direction of $\boldsymbol{k}$. This is related to the fact that velocity of sound is anisotropic. It has observable consequences in the form of the fluctuations of the order parameter above $T_c$ and the suppression of critical fluctuations. The points of mathematical difficulty in the theory we shall have to watch arise from these two features, i.e. the volume term in (1.1) and the elastic anisotropy, both contributing a singularity at $\boldsymbol{k} = \boldsymbol{0}$.

Incidentally, the strain-mediated interaction does produce a genuine phase transition without the addition of any Coulomb or nearest-neighbour interaction. In fact the behaviour of the order parameter $Q(T)$ follows rather well that derived from the Bragg–Williams (mean-field) theory, as might be expected from the infinite range of the $J_Z$ part of $J(R_{ij})$ (1.1). This is shown in figure 2, which was obtained from a computer simulation on a model of the type shown in figure 1, as described in more detail in [9].

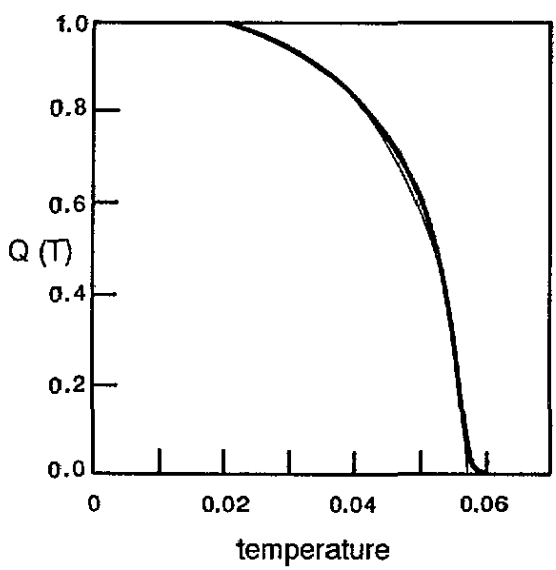


**Figure 2.** The order parameter $Q$ as a function of temperature $T$ in a computer simulation of a system with interaction $J(R_{ij})$ in the manner of figure 1 (heavy line). It has the normal form of a structural phase transition and in fact follows mean-field theory (Bragg–Williams approximation, light line).

While the previous work focused on the interaction $J$ [1], the purpose of the present paper is to add the entropic terms to $J(\boldsymbol{R})$ or $J_k$ so as to develop in section 2 a Landau–Ginzburg type of free energy functional $G_{LG}$. This can then be used to give a theory of various thermodynamic effects associated with the ordering phase transition, some of which will be discussed here and others only mentioned briefly. In particular we will consider in section 3 the strong fluctuations above $T_c$ that result in the tweed texture on cooling through $T_c$. In section 4 we will treat the shape of domain boundaries and how far the traditional Landau–Ginzburg theory can be taken over. In section 5 we will analyse the critical fluctuations near $T_c$ and the existence and magnitude of any Ginzburg interval $\Delta T_G$ of non-classical fluctuations around $T_c$. The other main consequence of a strain-mediated interaction is its effect on the kinetics of (dis)ordering. Especially in the ferroelastic case (1.1), the infinite range of the Zener term means each cell 'knows what every other cell is doing', so that ordering proceeds in a rather uniform manner over a rather large domain instead of the traditionally discussed nucleation and growth mechanism [3,4]. As a result of the rather homogeneous (dis)ordering one can develop a rate theory for the process, even far from equilibrium [7–9].

In [1] we have shown, however, that the interaction (1.1) results in a highly *non-local* form of the internal energy of a strain-coupled system

$$E = E_0 - \frac{1}{2}\sum_{ij} J(\boldsymbol{R}_{ij})Q(\boldsymbol{R}_i)Q(\boldsymbol{R}_j). \tag{1.3}$$

This cannot be expressed in local form because the summation (1.3) becomes an integral, which is only marginally convergent with the interaction (1.1), so the energy of a domain or an ordering embryo above $T_c$ is strongly shape dependent. Note that the first term in (1.1) diverges logarithmically when integrated over a cone, although it adds up to zero when averaged over all directions. This consideration incidentally gives an insight into the existence of very strong embryonic 'tweed'-like fluctuations above $T_c$ and the development of a tweed texture when quenched below $T_c$. In any case the development of a Landau–Ginzburg free energy functional in section 2 is not as straightforward as in the conventional theory with short-ranged interactions [9].

## 2. Formulation of the Landau free energy

We have already given in section 1 the bare essentials of our model. We have a local order parameter $Q(\boldsymbol{R}_i)$ in the cell centred at $\boldsymbol{R}_i$, and the local strain field around $\boldsymbol{R}_i$ due to the ordering process results via elastic propagation in the interaction $J(\boldsymbol{R}_i - \boldsymbol{R}_j)$ between cells, the energy $E$ being given by (1.3) [1]. Our first task is to write down the corresponding Landau free energy $G_{LG}$ and the second to summarize its characteristics.

To obtain $G_{LG}$ we need only add the entropy term to the energy (1.3) in the usual manner of the Bragg–Williams theory of phase transition [10,11]:

$$G_{LG} = G_0(T) - \frac{1}{2}\sum_{i,j} J(\boldsymbol{R}_{ij})Q(\boldsymbol{R}_i)Q(\boldsymbol{R}_j) + \sum_i k_B T\left[\frac{1}{2}Q(\boldsymbol{R}_i)^2 + \frac{1}{12}Q(\boldsymbol{R}_i)^4 + \dots\right]. \tag{2.1}$$

Here we have taken the entropy of an Ising spin in each cell in terms of the usual $\frac{1}{2}[1 \pm Q(\boldsymbol{R}_i)]\ln\frac{1}{2}[1 \pm Q(\boldsymbol{R}_i)]$ and expanded about the disordered state. If we have some

displacive variable in a double-well potential instead of an atomic ordering in each cell describable by an Ising spin, then the form of $G_{LG}$ remains the same but the numerical coefficients in the entropy term are altered.

It is more convenient to work with $Q_k$, $J_k$, the Fourier transforms of $Q(R_i)$, $J(R_{ij})$, in terms of which the energy and the free energy become

$$E = E_0 - \sum_k J_k Q_k Q_{-k} \tag{2.2}$$

$$G_{LG} = G_0 + \sum_k (k_B T - J_k) Q_k Q_{-k} + O(Q^4) \tag{2.3}$$

where the higher-order terms are the same as in (2.1) and (2.2).

The special features due to a strain-mediated interaction all stem from the behaviour of $J_k$, which was developed in detail in [1] and which we now summarize. In [1] we started with the simplest model of strain coupling, namely with $Q(R_i)$ coupled linearly by a set of forces $F(R - R_i)$ to the displacements $u(R)$ of nearby atoms at $R$:

$$H = \frac{1}{2} \sum_{RR'\alpha\beta} u_\alpha(R) \Phi_{\alpha\beta}(R - R') u_\beta(R') - \sum_{RR'\alpha} F_\alpha(R - R_i) u_\alpha(R) Q(R_i). \tag{2.4}$$

Here the first term is the usual energy of harmonic distortion of a lattice (phononic contribution), and the second represents a bilinear coupling. The indirect coupling via the strain fields can be calculated explicitly. Here we are only interested in the long-wavelength behaviour, which has a form largely determined by symmetry. For ferroelastic transitions, to which we shall confine ourselves from now on, unless explicitly states, $J_k$ is given by

$$\begin{aligned} J_k &= \Omega_c C_{\alpha\beta\gamma\lambda} e^0_{\alpha\beta} e^0_{\gamma\lambda} - P \qquad k = 0 \\ J_k &= F^\alpha_k G^{\alpha\beta}_k F^\beta_k - P \qquad k \neq 0. \end{aligned} \tag{2.5a}$$

In (2.5) $C_{\alpha\beta\gamma\lambda}$ are the elastic constants of a crystal; $\Omega_c$ is the volume of a unit cell; $e^0_{\alpha\beta}$ is the microscopic strain tensor defined by the equations

$$C_{\alpha\beta\gamma\lambda} e^0_{\gamma\lambda} = \lambda_{\alpha\beta} \tag{2.5b}$$

$$\lambda_{\alpha\beta} = \frac{1}{2\Omega_c} \sum_R F_\alpha(R - R_i) \cdot (R - R_i)_\beta + (\alpha \leftrightarrow \beta). \tag{2.5c}$$

The lattice Fourier transforms of the forces $F$ and the inverse matrix of the force constant $\Phi^{-1}$ define $F_k$ and the lattice Green function $\mathbf{G}_k$ entering the expression (2.5$a$).

The specific features due to strain-mediated coupling are described in detail in [1]. $J_k$ has two types of singularity at $k = 0$. Firstly, the long-range nature of $J(R)$ results in a very peculiar long-wavelength behaviour of $J_k$

$$J_k = d(n) - g(n)k^2 \tag{2.6}$$

where $n = k/k$ is a directional unit vector. Thus $d(n)$, the limit $J_{k\to 0}$, is anisotropic and depends strongly on the direction $n$ in which the limit is approached. It stems from the fact

that the lattice Fourier transform of the spin-lattice forces, $F_k^\alpha$, and the lattice Green function, $G_k^{\alpha\beta}$, entering expression (2.5*a*) for $J_k$ have the following long-wavelength behaviour:

$$F_k^\alpha \propto \lambda_{\alpha\beta} k^\beta \qquad G_k^{\alpha\beta} \propto \Delta_{\alpha\beta}(n)/k^2$$

where $\lambda_{\alpha\beta}$ is given by (2.5*c*) and $\Delta_{\alpha\beta}(n)$ can be expressed through elastic constants. Thus, the dependence of $J_k$ on the modulus of momentum disappears in zeroth order resulting in the behaviour (2.6).

Secondly, there is a delta-function at $k = 0$ from the Zener–Eshelby term $J_Z$ in (1.1). Thus, in general, $J_{k=0}$ is different from the limit $k \to 0$ along any direction (figure 3) and we have the fundamental property

$$J_{k=0} \geqslant d(n) \qquad \text{for any } n. \tag{2.7}$$

However, in some cases $J_{k=0}$ is equal to $d(n)$ for certain symmetry directions, and these are the 'soft' directions where from (2.3) the fluctuations have a low free energy, i.e. their amplitude is enhanced. As usual, the mean-field expression for the critical temperature for ferroelastic systems is given by the value $J_k$ at $k = 0$:

$$k_B T_c = J_{k=0}. \tag{2.8}$$

It is very important to note that the right-hand side of (2.1) cannot be represented in a local form, as can be seen in terms of real space from the long-range behaviour (1.1) of $J(R_{ij})$. This results in there being a strong shape dependence of the energy of the domains in a textured ferroelastic system, as discussed following (1.3).

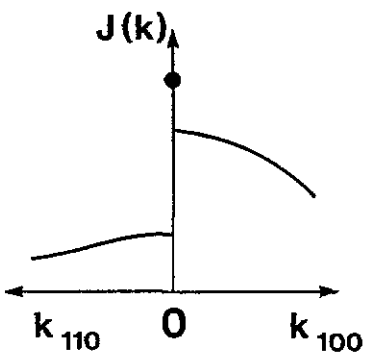


**Figure 3.** The most general form of the interaction $J_k$ in reciprocal space. The value $J_{k=0}$ is larger than the limit $k \to 0$ in any direction.

In order to discuss the form of $J_k$ further, it is necessary to be more specific. It was shown in [1] that one must distinguish three ferroelastic cases. For antiferro-coupling *there is a weaker singularity around* $k = 0$ *which in any case is rather irrelevant because* ordering takes place around some point $k_0$ on the Brillouin zone boundary where $J_k$ is an analytic function of $k$: the situation is completely analogous to that in the nearest-neighbour Ising model and the conventional Landau description of the phase transition.

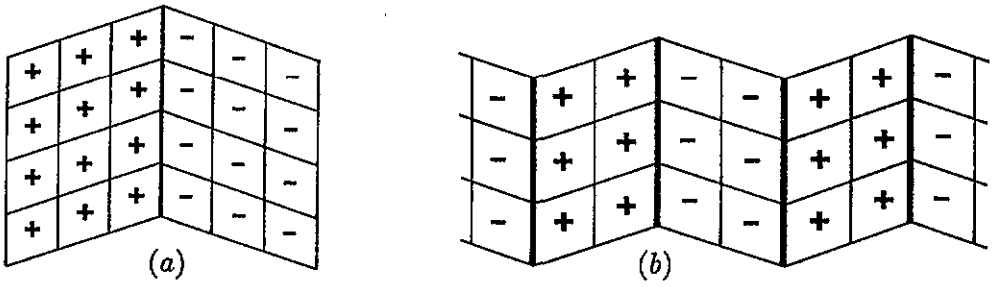


**Figure 4.** Domain boundaries for ferroelastic transitions with the $e_{xy}$ type of shear: (a) a single boundary; (b) a periodic array with wave vector $k$ in the (100) direction.

Antiferroelastic coupling occurs when local order $Q(R_i)$ sets up a surrounding stress field that has a different symmetry from that of any macroscopic strain.

Among ferroelastic couplings, one must distinguish three cases as shown in [1]. The most general case is that of figure 3 where $J_{k=0}$ is larger than the limit $d(n)$ in all directions $n$: this case is exemplified by a coupling of the $Q(R_i)$ to a volume strain of the cell or a tetragonal $2zz-xx-yy$ type of strain which we shall refer to as cases $F$(vol) and $F(2zz-xx-yy)$ respectively. Note that we are only considering a scalar order parameter $Q(R_i)$: the theory can be extended to multicomponent order parameters as discussed in [1]. When the coupling of $Q(R_i)$ to the lattice has the symmetry of a strain, domains with order parameter +1 and −1 show opposite macroscopic strains as in figure 4 and a macroscopic domain boundary between them has to satisfy certain geometrical conditions [13] for the lattice planes on the two sides to join up coherently. In the general case this is not possible for any direction, but with a strain of non-zero $\epsilon_{xy}$ (our $F(xy)$ case) such boundaries are possible perpendicular to the (100) and (010) directions (figure 4). Indeed one can form whole arrays of such boundaries (figure 4(b)) without any special strain of the cells on the boundaries, i.e. with zero energy cost, and the same is true of analogous sinusoidal modulations of the order parameter. Thus in the $F(xy)$ case $J_k$ is constant along two 'ridges' with $k$ along the soft (100) and (010) directions, and is equal there to the value $J_{k=0}$ governing $T_c$ (figure 5). Finally our $F(xx-yy)$ case with $xx-yy$ strain coupling illustrates the situation where the geometrical compatibility relations [13] do allow coherent boundaries, in this case perpendicular to the (±1, 1, 0) directions, but they involve extra distortions of the cells in and near the boundaries. In this case $d(n)$ along these ridge directions is again equal to $J_{k=0}$ but the $g(n)$ in (2.6) is non-zero (figure 6).

The profile of $J_k$ in ferroelastic cases therefore consist of 'ridges' along 'soft' directions and 'valleys' along 'hard' directions. If and only if Sapriel's compatibility relations are satisfied, $J_k$ along the ridge comes in to $J_{k=0}$, i.e. we have

$$J_k(\text{ridge}) = J_{\max} - gk^2 \tag{2.9}$$

exemplified by our $F(xx-yy)$ case. The $F(xy)$ case is very degenerate with $g(n) = 0$ along the 'ridge' directions. $J_k$ in figures 5 and 6 was calculated with the model of [1–3] in which local order in the cell at $R_i$ produces unit forces $F$ in appropriate directions at the eight corners of the cell (figure 1). The elastic medium represented by the dynamical force matrix $\Phi_{\alpha\beta}$ in (2.4) consists of a simple cubic lattice where nearest and next-nearest neighbours are connected by springs with force constants $K_1$ and $K_2$ respectively.

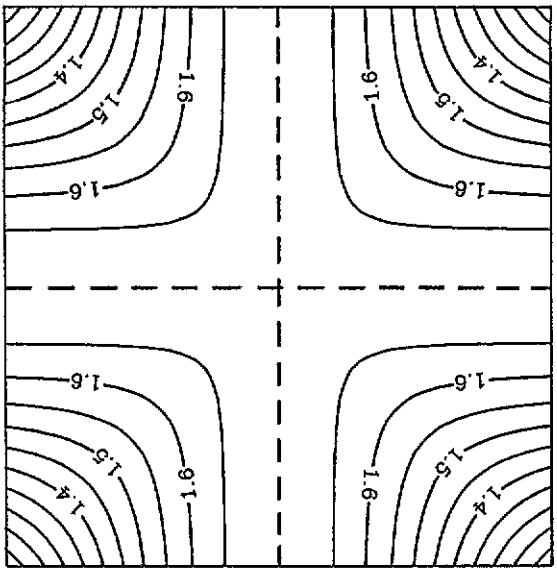


**Figure 5.** The interaction $J_k$ in the $k_x$, $k_y$ plane for the ferroelastic model of figure 4.

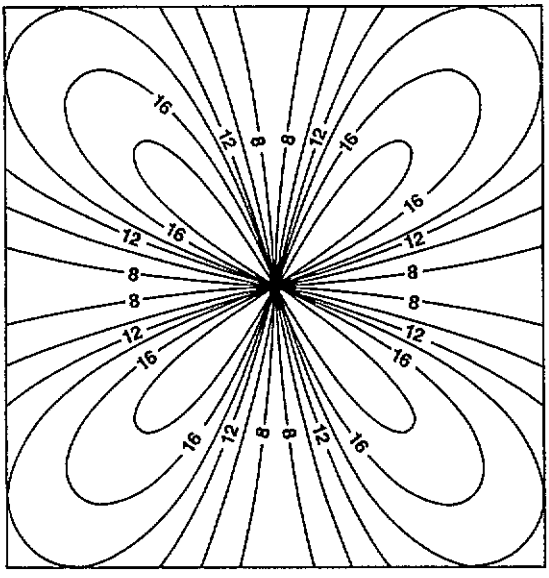


**Figure 6.** The interaction $J_k$ in the $k_x$, $k_y$ plane for the ferroelastic model $F(xx-yy)$ with the $e_{xx}-e_{yy}$ type of strain.

## 3. Application to tweed embryos

Tweed texture appears as a metastable structure on cooling a material through the transition temperature $T_c$, with many fine lamellae domains lying in two perpendicular planes. Since it appears below $T_c$, it is normally thought of purely as a product of the ordering kinetics. This is incorrect. Certainly the *development* of the tweed with time is determined by the

kinetics, but its *origin* lies in the tweed embryos, which are already very strongly present as normal thermal fluctuations in the material at all temperatures well above $T_c$. Figure 7 shows the result of a computer simulation (detailed below) at $T \simeq 2T_c$ frozen at one instant of time. We see that the material is a dense medium of tweed embryos everywhere, not just a few nuclei here and there. The same has been found in other similar simulations. Naturally the embryos are even stronger at $T$ near $T_c$, and then on cooling below $T_c$ the metastable tweed structure simply starts as a freezing in of the embryos present above $T_c$. Subsequently the domains sharpen up and coarsen in time, as described elsewhere [14, 15].

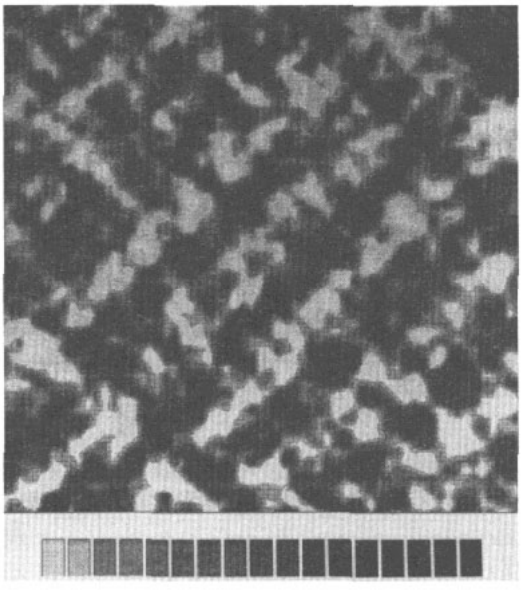

**Figure 7.** A snapshot of the fluctuations at high temperature $T = 1.7T_c$ in a computer simulation of the model of figure 6, showing the value of the strain order parameter $Q(R)$ in one layer of $64 \times 64$ cells of the simulation sample. Note the strongly developed tweed-like microdomains.

The present paper is concerned with fluctuations, and the purpose of this section is to show quantitatively that the dense medium of embryos above $T_c$ as in figure 7 can be explained more or less completely in terms of the classical theory of fluctuations based on the free energy developed in section 2. The first point is that it is unusual to have such strong fluctuations of the order parameter so far above $T_c$: note that the order parameter $Q(R)$ is near $\pm 0.5$ inside some microdomains (figure 7). The difference from e.g. a nearest-neighbour Ising model lies in the form of $J_k$, being large along ridges in $k$ space (section 2). The second point is to explain the geometry of the embryos, i.e. the extreme anisotropy of the microdomains. There are, roughly speaking, two length scales in figure 7, the *width* of the microdomains and their length, and it is the difference between these that gives the characteristic tweed effect.

Our model, both for theoretical analysis and for computer simulation, follows that described in [1–4]. We consider a simple cubic array of cells (lattice constant $a$) with 'atoms' at the corners connected by springs of strength $K_1$ and $K_2$ to first and second neighbours. Inside each cell $i$ is an Ising pseudospin $Q_i = \pm 1$ to represent the ordering inside that cell, whatever it may be. When $Q_i = +1$ a set of forces $F(R - R_i)$ act at

the eight corners of the cube $i$ to represent the local stresses on the surrounding material set up by the ordering in cell $i$, and of course forces $-F(R-R_i)$ when $Q_i=-1$. The 'atoms' at the corners of the cell can suffer displacements $u(R)$ and hence propagate the effect of $Q_i$ through the material to distant cells at $R_j$, causing an effective strain-mediated interaction $J(R_{ij})$ or $J_k$ in Fourier transform. The model is a discrete version of that used by Parlinski *et al* [14, 15] and various tests showed that the differences between the results of computer simulations are minor. The complete theory of $J_k$ is given in [1] and the results in figures 5 and 6 were calculated for sets of forces having the symmetry of $e_{xx}-e_{yy}$ and $e_{xy}$ shears respectively and producing such shears on ordering. We refer to them as our $F(xx-yy)$ and $F(xy)$ cases where $F$ denotes that they result in ferroelastic transitions. The computer simulations were carried out on samples mostly of $64\times64\times7$ cells with free boundary conditions. Increasing the sample size did not alter the results. The system was equilibrated using the Glauber dynamics for the pseudospins $Q_i$. After each new configuration the 'atoms' were relaxed to their new (static) equilibrium positions using Newtonian dynamics, with a strong frictional force to speed equilibration. It was shown in [1–4] that with our harmonic springs the thermal agitation of the 'atoms' about these equilibrium positions is completely decoupled from the interaction $J$ and hence is written out of the computer code. The simulations were implemented on the DAP AMT computer in Cambridge. $J_k$ was calculated as the interaction between the $Q(R_i)$ as defined.

To give a theory of the embryonic domains above $T_c$ and their dimensions we now follow the conventional theory of fluctuations. Each $Q_k$ is considered as an independent Gaussian fluctuation, resulting in a free energy of $\frac{1}{2}k_BT$. We then obtain from the Landau free energy (2.3) the correlation function

$$S_k=\langle Q_kQ_{-\underline{k}}\rangle=k_BT/(k_BT-J_k) \tag{3.1}$$

where $\langle\ldots\rangle$ denotes the thermodynamic average. From (3.1) $S_k$ has a butterfly shape similar to $J_k$ with four ridges in the $(\pm1,\pm1,0)$ directions for the $F(xx-yy)$ case, as observed in simulations. It reflects the extreme anisotropy of $J_k$ at low $k$ discussed in section 2 with its ridges along the $(\pm1,\pm1,0)$ directions, which in turn reflects the ease of forming domain walls perpendicular to these directions (see section 2 and [1], [3] and [4]).

A quantitative comparison of (3.1) along a ridge with $S_k$ from a simulation of $1.7T_c$ is shown in figure 8. The $S_k$ from simulations (figure 8(a)) is notoriously noisy [16] but with that reservation the agreement with (3.1) (figure 8(b)) is satisfactory and confirms our whole argument about the bulk of tweed embryos above $T_c$ being normal thermodynamic fluctuations (figure 8). The strength of the fluctuations can be gauged from the fact that the local strain in the microdomains is typically $0.5e_0$ where $e_0$ is the spontaneous strain (2.5*b*) of the perfectly transformed material at 0 K. At $1.3T_c$ the data were noisy. We also now see deviations from (3.1), in particular the reduction in $S_k$ below (3.1) at low $k$ along the ridge (figure 8(a)). This was found in several independent runs and we believe is not noise: it may be due to finite sample size and/or saturation effects [16]. The possible importance of saturation effects can be understood qualitatively by noting that the local spontaneous strain is even larger than that at $1.3T_c$ noted above. The saturation effect at low $k$ was even stronger in the two-dimensional simulations of Parlinski *et al* [14, 15].

We can analyse figures 7 and 8 one step further to derive the length scales. For $k$ in the region of one of the four ridges, we can write approximately

$$J_k\simeq k_BT_c\left(1-\xi_1^2k_r^2\right)\left[1-\xi_2^2\left(k_r\right)k_p^2\right] \tag{3.2}$$

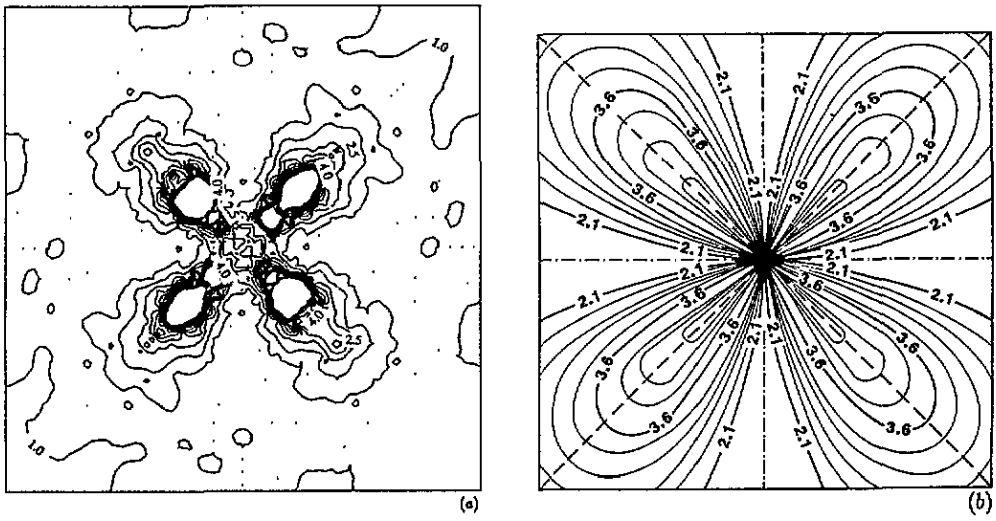


**Figure 8.** The correlation function $S_k$ in reciprocal space for the tweed-like fluctuations above $T_c$: (a) from the simulation in figure 7; (b) from the simple theory of (3.1).

where $k_r$ and $k_p$ are respectively the components of $k$ along the crest of the ridge and perpendicular to it. On substituting (3.2) into (3.1) and Fourier transforming into the correlation function $S(R)$ in real space, we can interpret $2\xi_1$ as the width of a microdomain and obtain from figure 8 a value of order 1.5 lattice spacings in a typical run at $1.7T_c$. Similarly the (narrower) width of the ridge gives the (longer) length of the domains. An analysis of the theory of $J_k$ [1] shows that $2\xi_2(k_r)$ is not a constant along the ridge if one makes a fit of the form (3.2), but varies with $k_r$ as already indicated in (3.2). There is therefore *no unique length scale* for the length of the microdomains but we may take a typical value of $k_r = 0.25/a$ along the main part of the ridge and obtain a length of order $\xi_2 \simeq 7a$ again in agreement with figure 7. Note there is no new physics in going from $S_k$ to the real-space picture of figure 7: it is largely a matter of Fourier transformation, and our analysis via (3.2) is a useful check in view of the somewhat complicated form of figures 7 and 8. Moreover from (3.1) and (3.2) we expect $\xi_1 \sim |T - T_c|^{-1/2}$, which fits roughly to a comparison of simulations at $1.7T_c$ and $1.3T_c$.

We conclude that the width of the embyronic microdomains is determined by the curvature of $J_k$ along the crest of the ridge, and the length of the domains, less well defined in figure 7, is determined by the width of the ridge in some general sense. This picture is confirmed by two further simulations. Figure 9 shows order parameter fluctuations under the same conditions as in figure 7 but now for the $F(xy)$ model. Recall from section 2 that $J_k$ is flat along the crest of the ridge in this case because it costs zero energy to form any number of domain walls (figure 4). Thus $\xi_1$ in (3.2) becomes zero and with width of the domains has indeed shrunk to one or two lattice spacings in figure 9. On the other hand in the $F$(tetrag) case with tetragonal strains of symmetry $2zz{-}xx{-}yy$, no macroscopically coherent domain walls are possible by Sapriel's compatibility relations: we are only considering the situation of domains with positive and negative strains, not that of a multicomponent order parameter with tetragonal shears around the $x$, $y$ and $z$ axes. The conditions for coherent macroscopic domain walls between regions of strain $e^{(1)}$ and $e^{(2)}$ are

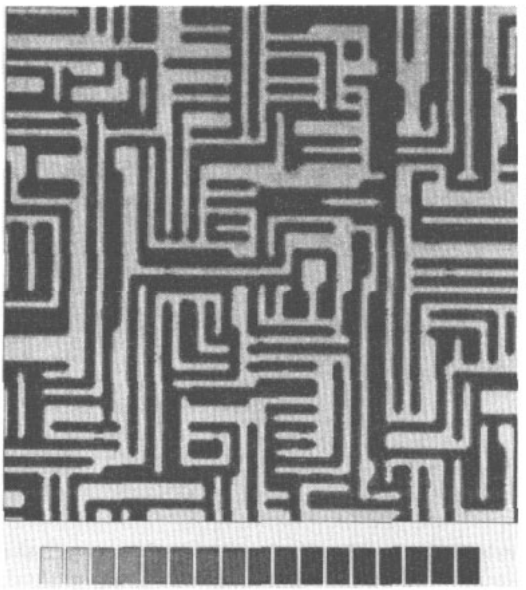

**Figure 9.** The tweed-like fluctuations under similar conditions to figure 7 for the ferroelastic model of figure 4 with $e_{xy}$ strains, with the width of the microdomains only one or two lattice spacings.

$$\det\left(e_{\alpha\beta}^{(1)} - e_{\alpha\beta}^{(2)}\right) = 0$$

and

$$\mathrm{Tr}\left(e_{\alpha\beta}^{(1)} - e_{\alpha\beta}^{(2)}\right) = 0 \tag{3.3}$$

where in our case $e^{(2)} = -e^{(1)}$. It is easy to verify that $2zz{-}xx{-}yy$ shear does not satisfy (3.3). This fact is reflected in the behaviour of $J_k$, which does not reach the value $J_{k=0}$ in the limit $k \to 0$ along any direction (figure 3). Even small domain boundaries cost a substantial energy and are suppressed in the fluctuations as shown in figure 10.

Returning to the classic case of tweed in figure 7, we observe that there appears to be no distinction between twice the thickness of a domain wall and the width of a domain, nor is any expected from (3.1) and (3.2). However the situation changes on quenching the system rapidly to below $T_c$ [1, 3, 4]. Initially in our simulations the general pattern of microdomains remains that in the fluctuations above $T_c$ before the quench, but the domain walls rapidly sharpen up to narrower boundaries in accordance with the theory of domain walls developed in the next section, thus introducing a third length scale. However we should add one caution: dimensionally speaking there is only one length scale in our theoretical model, namely the cubic lattice constant. There is no other physically determined length. All other relevant quantities are ratios such as $T/T_c$, the strain $e_0$ and elastic properties of the medium determined by $K_1/K_2$. The tweed texture might therefore involve a continuum of length scales, with those we have picked out being most significant.

The above discussion has focused largely on an analysis in $k$-space. However one can obtain a physically equivalent picture from $J(R)$ in real space. $J(R)$ is extremely

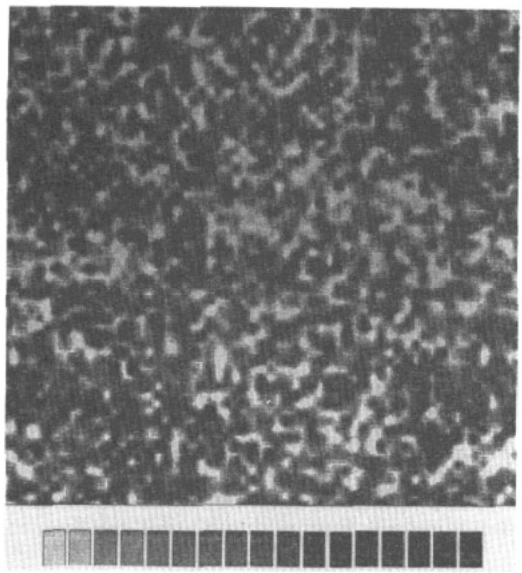

**Figure 10.** Fluctuations under similar conditions to figures 7 and 9 for the ferroelastic model with tetragonal shears of type $2e_{zz}-e_{xx}-e_{yy}$. There are no tweed-like microdomains because of the higher energy cost in forming domain walls, due to not satisfying the compatibility relations (3.3) for coherent boundaries.

anisotropic, with the $Y_{4m}$ terms in (1.1) dominating [1]. For example in the $F(xx-yy)$ case, $J(R)$ is ferroelastic in sign in the $(\pm1, \pm1, 0)$ directions and antiferroelastic in the $(\pm1, 0, 0)$, $(0, \pm1, 0)$ directions. Moreover their long range means that they add up in one direction. This accounts for the shape of the thin slab domains parallel to the $(\pm1, \pm1, 0)$ directions. The real-space picture also explains quantitatively why the fluctuations above $T_c$ are so strong. The anisotropic part of $J(R)$ averages to zero, so that $T_c$ is determined by the rather weaker uniform part $J_Z$.

In conclusion, therefore, the fluctuations seen as tweed embryos above $T_c$ are much stronger than one is normally accustomed to in phase transitions, e.g. in a nearest-neighbour Ising model, but there is nothing mysterious about them. They can be accounted for quantitatively by traditional Ornstein–Zernike theory until close to $T_c$ it breaks down as the fluctuations become too strong. The picture in real space also shows why the forces governing the shape of fluctuations are large compared with $k_BT_c$.

## 4. Application to domain boundaries

Throughout this section we will consider planar domain boundaries of infinite extent at temperatures below $T_c$. This issue is, to what extent can the traditional Landau–Ginzburg theory of the wall width and wall energy based on the free energy functional $G_{LG}$ be taken over into our more complicated situation? We start with the form (2.3) for $G_{LG}$ and substitute the form (2.6) for $J_k$ in the continuum limit to obtain

$$G_{LG} = G_0 + \sum_k \Big[k_BT - d(n) + g(n)k^2\Big] Q_k Q_{-k} + O(Q^4) \tag{4.1}$$

where $k$ is always in the direction $n$ perpendicular to the boundary, and where the fourth-order terms are the same as in (2.1). As usual we would like to interpret $ik$ as the gradient operator so that (4.1) becomes the conventional form for the free energy per unit area of wall:

$$G_{LG} = G_0 + a^{-1}\int dx\left\{\frac{1}{2}\left[k_B T - d(n)\right]Q^2(x) + \frac{1}{12}k_B T Q^4(x) + \frac{1}{2}g(\nabla Q)^2\right\}. \tag{4.2}$$

But we cannot do that here in general because $d(n) - g(n)k^2$ is not an analytic function of $k$. However, we can proceed with such a transformation in special cases satisfying two conditions: (i) that we are dealing with a physical case where $J_{k=0}$ is the same as the limit $k \to 0$ along some direction $n$, and (ii) that our boundary is perpendicular to such a direction. We then have in (4.2)

$$d(n) = k_B T_c \tag{4.3}$$

and (4.2) takes the usual Landau–Ginzburg form with the usual result

$$W = \left[g(n)/k_B(T_c - T)\right]^{1/2} \tag{4.4}$$

for the wall width and a profile of form

$$Q(x) = Q_0(T)\tanh\left(x/2^{1/2}W\right) \tag{4.5}$$

where $Q_0(T)$ is the thermodynamic value of the order parameter.

The important point is that the free energy functional (4.2) is formally minimized when $Q(x)$ far from the wall has the uniform value

$$Q(n) = \left[\left[d(n) - k_B T\right]/k_B T\right]^{1/2}. \tag{4.6}$$

This is only equal to the bulk thermodynamic value

$$Q_0(T) = \left[\left(T_c - T\right)/T\right]^{1/2} \tag{4.7}$$

when the condition (4.3) holds, i.e. when the conditions (i) and (ii) above are both satisfied. Otherwise the material formally has a free energy density distant from the wall higher than the bulk thermodynamic equilibrium value. The physical reason is that with a boundary not satisfying the compatibility relations (3.3) there has to be a non-zero lateral strain to make the lattices of the two sides match parallel to the boundary as illustrated in figure 11. Of course that would leave the material in an unstable state of strain away from the boundary, so that in reality it would break up into some kind of domain texture.

We need to add one gloss concerning the validity of our arguments. The development of the general theory in [1], clearly stipulated that the specimen had macroscopically a uniform strain, which rules out the treatment of a single domain wall as done here. However one can consider a regular or irregular array of parallel walls as in figure 4(b) and recover the

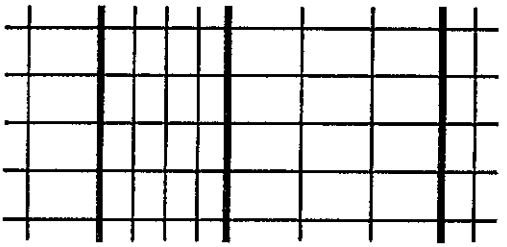

**Figure 11.** A domain boundary in the 'wrong' (100) direction for the model with $e_{xx}$–$e_{yy}$ shear. Coherent boundaries of low energy run in the (±1, 1, 0) direction as in figure 7. The (100) boundary shown requires additional volume strains to match the lattice planes across the boundary, resulting in a substantially higher energy.

results of the present section by considering all possible arrays and taking the limit as the density of walls tends to zero. In that sense (4.2) has a wider applicability for a wall of type (4.3) than the assumptions that went into it. However, one must not push one's luck: we have found the theory can produce inconsistent and spurious results if one ignores the original condition.

Finally we remark that in antiferroelastic systems there is no macroscopic strain, the compatibility relations (3.3) are irrelevant, we have $d(\boldsymbol{n}) = 0$, and $J_{\boldsymbol{k}}$ is analytic around the point $\boldsymbol{k}_0$ of the antiferroelastic phase transition. Thus a normal Landau–Ginzburg functional applies. The domain boundaries are irregular in shape and much more mobile.

## 5. Application to critical fluctuations

In this section we consider the build-up of critical fluctuations close to $T_c$. We do not calculate critical exponents but merely assess to what extent the Landau free energy is self-consistent in terms of fluctuations and how large the corrections are, using the standard theory [17, 18]. Long-range elastic forces are known to suppress critical fluctuations in systems with striction or having an acoustic instability. The discussion in previous sections shows that the physics of cooperative behaviour in ferroelastic systems with a strain-coupled order parameter is different, although there are some similarities to previously studied cases. In our cases the gap between a ferroelastic $J_{\boldsymbol{k}=\boldsymbol{0}}$ and the limit of $J_{\boldsymbol{k}}$ as $\boldsymbol{k} \to \boldsymbol{0}$ in all or nearly all directions clearly reduces the amplitude of fluctuations as is evident from (3.1).

We now follow the usual way of estimating Gaussian classical fluctuations to explore the possible classes of critical behaviour in strain-coupled systems [18, 19]. The correction to the heat capacity from the fluctuations contains integrals such as

$$\Delta C_p \sim \int \frac{\mathrm{d}^3 k}{(2\pi)^3} S_{\boldsymbol{k}}^2 \tag{5.1}$$

where $S_{\boldsymbol{k}}$ is the correlation function for fluctuations. For simplicity we confine ourselves to the region $T \gtrsim T_c$ in which case from (3.1) with the long-wavelength behaviour (2.6) of $J_{\boldsymbol{k}}$ we have an (Ornstein–Zernike) approximation quadratic in $\boldsymbol{k}$

$$S_{\boldsymbol{k}} = \langle Q_{\boldsymbol{k}} Q_{-\boldsymbol{k}} \rangle = k_B T / \left[ k_B T - d(\boldsymbol{n}) + g(\boldsymbol{n}) k^2 \right]. \tag{5.2}$$

It is easy to show using (2.5) that the function $d(n)$ entering (5.2) is extremal along some 'soft' directions in ferroelastic systems. In a typical case of the $F(xx-yy)$ coupling they are $[1, \pm 1, 0]$ as determined by a term proportional to $(n_1^2 - n_2^2)^2$, where $n_1$ and $n_2$ are the directional cosines in a basal plane [1]. Choosing one axis along a 'soft' direction in the basal plane, we can rewrite the expression for $S_k$ (5.2) in the following general form using polar coordinates in $k$-space (exact to within some proportionality constant):

$$S_k \propto \left[1/r_c^2 + \Delta^2 + a^2 \cos^2\theta + b^2 \sin^4 \Theta \sin^2 2\varphi + gk^2\right]^{-1} \tag{5.3}$$

where $r_c = [T_c/(T - T_c)]^{1/2}$ is the usual correlation length proportional to $W$ (4.4), $\theta$ and $\varphi$ are the polar and azimuthal angles, respectively, and $a$, $b$ and $g$ are the material constants expressed via elastic constants. Here we have neglected the unimportant angular dependence of $g(n)$ in (5.2). This form of correlator is analogous to that characteristic of the displacive phase transitions in ferroelectrics where a critical mode is coupled to the acoustic phonon [19].

It should be mentioned that $\Delta^2 \neq 0$ for $F$(vol), $F$(tetrag), and other couplings that do not obey the Sapriel conditions (3.3). This means that in those cases $S_k$ (5.3) is non-singular everywhere in $k$-space. In the $F(xx-yy)$ and $F(xy)$ cases $\Delta^2 = 0$ and we can deduce immediately that $S_k$ is singular only in four special directions in the basal plane given for the $F(xy)$ case by $\theta = \frac{1}{2}\pi$ and $\varphi = 0, \pi/2, \pi$ and $3\pi/2$. All these directions contribute equally to the fluctuation correction to the specific heat (5.1). Now the integral (5.1) can be easily estimated near the critical point, with the following results.

(i) Ferroelastic systems having no domain boundaries satisfying the compatibility relations (3.3) such as $F$(vol) and $F$(tetrag) so that $\Delta^2 \neq 0$: $\Delta C_p$ is convergent as a smooth function of temperature, so Landau theory is self-consistent, i.e. correct.

(ii) Ferroelastic systems such as $F(xx-yy)$ having a set of domain boundaries satisfying the compatibility relations (3.3), but with the boundary having a non-zero energy and $J_k$ a curvature along the crest of the ridge: $\Delta C_p$ is convergent and Landau theory is again correct. We have the weak singularity

$$\Delta C_p \propto |T - T_c|^{1/2}. \tag{5.4}$$

(iii) Ferroelastic systems such as $F(xy)$ with domain boundaries satisfying the compatibility relations (3.3) and costing zero energy as in figure 4, so the ridge of $J_k$ has constant height: $\Delta C_p$ diverges with

$$\Delta C_p \propto |T - T_c|^{-1} \tag{5.5}$$

and Landau theory fails near $T_c$. It should be noted that short-range forces, which are always present in the system, will give $J_k$ on the ridge some curvature and hence suppress the divergence of (5.5), giving the more usual behaviour of (5.4).

(iv) Antiferroelastic coupling with order parameter $Q_k$ at a point $k_0$ on the Brillouin zone boundary: $\Delta C_p$ diverges with

$$\Delta C_p \propto \left(T - T_c\right)^{-1/2} \tag{5.6}$$

and there are the same types of correction to Landau theory as for the nearest-neighbour Ising model. Landau theory fails within the Ginzburg interval around $T_c$.

We conclude that the general formulation of Landau theory for the phase transition is valid for almost all ferroelastic cases. The reason is very general: the involvement of elastic forces makes the effective interaction infinitely ranged, which suppresses critical fluctuations [18, 19]. The mechanism does not operate for antiferroelastic transitions. We are not concerned here, therefore with the calculation of critical exponents. The related case of dipolar ferroelectrics was studied in great detail by renormalization group analysis in [20, 21], and critical fluctuations were shown to grow strong enough to destroy the Landau theory very close to $T_c$.

Another class of models, also different from what we have discussed here, is posed by the Ising-like models on a compressible lattice (see [22–26] and references therein) where strain is coupled to the square of an order parameter (quadratic striction). The critical fluctuations always build up to the point where they drive phase transition to be discontinuous (weak first order). Anisotropy may play a role once again in decreasing the discontinuity to well below observable level [23, 26].

The correlation function in real space is a very important characteristic of a transition and it is defined as a Fourier transform of the structure factor $S_k$ (5.2):

$$G(\boldsymbol{R}) = \int \frac{\mathrm{d}^3 k}{(2\pi)^3} \langle Q_k Q_{-k} \rangle \exp(\mathrm{i}\boldsymbol{k} \cdot \boldsymbol{R}). \tag{5.7}$$

At large $R$ the asymptotic behaviour of $G(\boldsymbol{R})$ is defined by the long-wavelength limit of $S_k$ (5.2). Let us discuss a typical $F(xx{-}yy)$ case. As follows from (2.5) and (2.6), the denominator in (5.2) vanishes only along special 'soft' directions in $\boldsymbol{k}$-space. This immediately results in a 'dipolar' asymptotic behaviour

$$G(R) \propto 1/R^3 \tag{5.8}$$

along 'soft' directions at $T = T_c$. At the same time $S(\boldsymbol{R})$ decays exponentially for all other directions even at the critical temperature. The reason for this lies in a less singular behaviour of the denominator in (5.2) in comparison with the situation in systems with finite-range coupling. In (5.2) the function $d(\boldsymbol{n}) = 0$ only in a few special *directions* in $\boldsymbol{k}$-space whereas $d(\boldsymbol{n}) \equiv 0$ in systems with finite-range coupling, and the integral (5.7) is determined mainly by areas close to these directions. This immediately leads to a $R^{-3}$ law instead of the usual $R^{-1}$ [11] decay of correlations in real space.

## References


[1] Bratkovsky A M, Salje E K H, Marais S C and Heine V 1993 *Phys. Rev.* B submitted
[2] Marais S C, Heine V, Nex C M M and Salje E K H 1991 *Phys. Rev. Lett.* **66** 2480
[3] Bratkovsky A M, Salje E K H and Heine V 1993 *Europhys. Lett.* submitted
[4] Bratkovsky A M, Salje E K H, Marais S C and Heine V 1993 *Phase Trans.* at press
[5] Zener C 1948 *Phys. Rev.* **74** 639
[6] Eshelby J D 1956 *Solid State Physics* vol 3 (New York: Academic) p 297
[7] Dattagupta S, Heine V, Marais S C and Salje E K H 1991 *J. Phys.: Condens. Matter* **3** 2963, 2975
[8] Salje E K H 1988 *Phys. Chem. Miner.* **15** 336
[9] Marais S C, Padlewski S and Salje E K H 1991 *J. Phys.: Condens. Matter* **3** 6571

[10] Stanley H E 1987 *Introduction to Phase Transitions and Critical Phenomena* (New York: Oxford University Press)
[11] Landau L D and Lifschitz E M 1980 *Statistical Physics* 3rd edn part 1 (Oxford: Pergamon)
[12] Giddy A, Dove M T and Heine V 1989 *J. Phys.: Condens. Matter* **1** 8327
[13] Sapriel J 1975 *Phys. Rev.* B **12** 5128
[14] Parlinski K, Heine V and Salje E K H 1993 *J. Phys.: Condens. Matter* **5** 497
[15] Parlinski K, Salje E K H and Heine V 1993 *Acta Metall. Mater.* **41** 839
[16] Sahni P S, Gunton J D, Katz S L and Timpe R H 1982 *Phys. Rev.* B **25** 389
[17] Levanyuk A P 1963 *Fiz. Tverd. Tela* **5** 1776
[18] Vaks V G, Larkin A I and Pikin S A 1966 *Zh. Eksp. Teor. Fiz.* **51** 361
[19] Levanyuk A P and Sobyanin A A 1970 *JETP Lett.* **11** 371
[20] Larkin A I and Khmelnitskii D E 1969 *Zh. Eksp. Teor. Fiz.* **56** 2087
[21] Aharony A and Fisher M E 1973 *Phys. Rev.* B **8** 3323
[22] Larkin A I and Pikin S A 1969 *Zh. Eksp. Teor. Fiz.* **56** 1665
[23] Bergman D J and Halperin B I 1976 *Phys. Rev.* B **13** 2145
[24] de Moura M A, Lubensky T C, Imry Y and Aharony A 1976 *Phys. Rev.* B **13** 2176
[25] Levanyuk A P, Minyukov S A and Vallade M 1993 *J. Phys.: Condens. Matter* **5** 4419
[26] Salje E K H and Vallade M 1993 *J. Phys.: Condens. Matter* submitted